Analytical Solutions and Case Studies on Stress-Dependent Corrosion in Pressurized Spherical Vessels

Cheng Huijuan Liu and Giuseppe Lacidogna *

Posted Date: 7 October 2023

doi: 10.20944/preprints202310.0407.v1

Keywords: pressure vessels; mechanically-assisted corrosion; variable boundary; analytical solution, stress; thickness; life

Article

Analytical Solutions and Case Studies on Stress-Dependent Corrosion in Pressurized Spherical Vessels

Cheng Huijuan Liu [1] and Giuseppe Lacidogna [2,*]

[1] Department of Mathematics, Aberystwyth University, Aberystwyth, Ceredigion, Wales, SY23 3BZ, UK; hul19@aber.ac.uk
[2] Department of Structural, Geotechnical and Building Engineering, Politecnico di Torino, 10129 Turin, Italy
* Correspondence: giuseppe.lacidogna@polito.it

Abstract: In this paper we overview all analytical engineering solutions for corrosion problems in pressure vessels delivered over the past 60 years. We briefly detail strengths and weaknesses of existing approaches, thus demonstrating the need for novel uniform corrosion analysis methods for both current and new applications. To complement the review, we also present a new analytical model allowing to estimate the lifetime of pressured elastic vessels with mechanically assisted corrosion. Both internal/external pressure and internal/external corrosion are captured and dissolution driven corrosion is also considered. The readily implemented method improves existing analytical approaches and is shown to be effective for thin and thick shells, as well as various loading and corrosion intensity and geometrical conditions.

Keywords: pressure vessels; mechanically-assisted corrosion; variable boundary; analytical solution; stress; thickness; life

1. Introduction

1.1. Corrosion research

Corrosion problems are common in pressure vessels of iron or steel in operation [1]. Chemical corrosion often occurs when they operate in dry environments. Conversely, in a humid (or water) environment, electrochemical corrosion occurs. These two types of corrosion will cause the loss of metal, which will in turn cause the container to crack, thus losing the stability/ultimate bearing capacity, shortening the service life, and greatly increasing the risk of various accidents and losses of the container. This problem also widely exists in other similar metal components, such as aerial vehicles [2], liquid hydrogen transportation pipelines [3], high temperature furnace devices [4], oil (gas) pipelines [5], chemical building components [6], marine platform components [7], marine submarines [8], and wearable device components [9,10]. They are used as air/land/sea infrastructure, equipment (devices), and other important military or pharmaceutical components.

1.2. Corrosion problems of pressure vessels

Regarding the corrosion of pressure vessels, many studies have focused on the specific development process of electrochemistry and the chemistry of metals [11–16]. And other researchers do not discuss the chemistry process, and all possible chemical reactions will be modeled with the help of some kinetic phenomenological laws. In this paper, we mainly focus on such phenomenological models since other type of models such as quantitative or analytical models were relatively lacking [17].

1.2.1. Phenomenological model

In the study of the phenomenological models, the corrosion process is usually regarded as uniform wear or dissolution of materials. In pressure vessels, this is often assisted by mechanical

 doi:10.20944/preprints202310.0407.v1

stress. In order to establish this model, the relationship between the corrosion rate and stress of the stressed component (a circular tube) [18] must therefore first be understood.

In [19] a linear model was proposed. It has some difficulties in expressing the effect of temperature on corrosion rate and mechanical stress. Considering the papers of Gutman et al., an Arrhenius' temperature model was introduced in [20–22] and, considered the classical thermodynamic laws, it was combined with a significant amount of experimental data. This model explained the relationship between environmental temperature, stress, and velocity, although has some problems in expressing the inhibition phenomenon in corrosion processes. In [20] a corrosion inhibition coefficient b was established, and adopted a mixed model with both polynomial and exponential terms. This model has been used to explain such corrosion inhibition phenomenon described above, but still has problems in explaining coating protection and rupture phenomena. Quadratic, cubic, and general cubic polynomial models respectively where proposed in [23]. These models have achieved the purpose of improving the description of existing experimental data and phenomena. They also have difficulties in expressing of threshold stress explicitly (including temperature) and in capturing the phenomenon of coating breakage.

Recently, the idea advanced in [23] is to introduce a stress threshold quantity into the model explained in [24], proposing a segmented corrosion model. However, it gives some results inconsistent with experimental phenomena when describing vessel corrosion problems with small stresses. In order to improve the above models, Gutman in 2016, based on the model [20] made a new one. Even it achieves the purpose of simultaneously describing the relationship between media activation energy, however, it is difficult to characterize the mechanical stress induced by temperature and then hard to describe its interaction with corrosion rate. Moreover, it may have difficulties in describing some experimental phenomena consistently. Regard to this problem, in [25] was introduced the temperature T_j, along with a threshold temperature T_j^{th}, plus an empirical parameter, β_i/β_o, into the model already presented in [26]. However, this parameter lacks of a clear physical interpretation. This last model [25] enables to describe the effect of thermal stress on corrosion rate and mechanical stress and conclude the monotonical effect of temperature difference between the outer and inner surface on corrosion rate and lifetime. However, it may have some computational difficulties for a case with a temperature larger than the temperature threshold.

1.2.2. Experimental research and data

Most phenomenological models described above did not provide related experimental validation. However, before these phenomenological models were proposed, a large amount of experimental data had been accumulated [20–22]. By reviewing the experimental research, we obtained effective experiments and their data from these works. Some of them have direct or indirect contributions (relationships) to several corrosion models successively proposed by Gutman's team. If these data can be employed properly to verify the corresponding corrosion model, the lack of current model validation will be improved.

1.2.3. Theories on corrosion lifetime (including failure criteria)

Existing shell stresses distribution equations

The accurate expression for the stress distribution (mechanical stress) on the sphere shell in the absence of temperature effects is Lamé formulas. Researchers always adopted the formulas of this equation with different assumptions (even including adding some terms, such as temperature) in different periods to obtain an analytical solution. In [19] such a stress distribution equation is proposed with a constant average diameter. In works of [27,30–32], the average diameter is replaced by the mid-surface radius r_c but still constant. In [26], based on Lamé formulas, new assumptions where introduced but poorly performing in mathematical operations (say Taylor expansion) with intermediate variable, η, less than or close to1.0. In [31] the mid-plane radius r_c was introduced into the first-order Lamé stress distribution equation. From the conclusions, an analytical solution was obtained that is as simple as the ones based on Laplace's Law, but with better accuracy. However, it

is difficult to describe the change of temperature stress on mechanical stress and corrosion rate. The model [25] was further improved by introducing the outer/inner radius ratio η and adding the temperature term. It has a little difficulty in expressing the effect of the inner and outer temperature values on the stress, respectively and also adds further complexity in implementation.

In summary, the key to achieve a better one model is to obtain a new analytical solution expressed by a new proper intermediate variable. For example, it will be possible to implement using the analytical solution based on x proposed in this paper.

Analytical relationship between vessel stress/thickness and time

The first is a solution based on Laplace's Laws such as built in [32]. It uses a stress distribution format expressed as a constant midplane radius. There are still difficulties in a broader range of applications and better accuracy in such applications. The second one is adopted in [31], which can be applied in a broader range and, simultaneously, ensures better accuracy. When used for shells as medium and thick shells, it is difficult and laborious to maintain a sufficient accuracy.

Recently [34] used the Southwell plot method, an estimation method is proposed for the critical thickness, critical life and critical stress of the shell, while the accurate failure criterion is avoided.

Failure criteria for further life problems (or critical stress or critical thickness) and its assumptions.

Researchers have proposed different failure criteria to study pressure vessels' corrosion problem (life problem), and they have various forms [17,19,22,26–33,35]. But when these stressed shells fail under the action of corrosion as well as force or pressure, their critical state will move in both space and time. However, if we want to find it precisely in time and space, there are still some difficulties, even though [35,36] has discovered this phenomenon and [25] redefines failure (lifetime).

1.3. Aspects requiring further analysis

Here we briefly detail strengths and weaknesses of existing approaches:

* It is challenging to improve (or create a new model) the current corrosion kinetic models based on the existing amount of test data.

One reason is a restricted amount of data from real engineering applications required to verify or improve the validity of those models used in the corrosion problem of pressure vessels. Another is the huge money and time cost of the data collection for shells generally with a long lifetime.

* The assumptions of the stress distribution equation need to be further optimized.

These simplified stress distribution equations, based on Lamé formulas or Laplace laws, are not perfect. For some, there are many assumptions, resulting in a decrease in accuracy or a narrow range of applications. Some, with few assumptions, make it difficult to obtain an analytical solution that is easy to program or friendly to engineering applications.

* Delivering difficulties of existing analytical methods.

* New applications (beyond pressure vessels) urgently need more efficient and easy-to-program analytical methods.

In general, we still lack an analytical solution that is simple enough in form that can analyze both thin and thick shells, adapt to complex working conditions, and maintain accurate and rapid expressions. And the need is increased by vessels becoming more advanced and complex in industry and other related land or sea infrastructure components.

1.4. Suggested improvement in analysis of the vessel corrosion problems

After the previous considerations on the current research situation，we will seek to improve the analytical theory of general corrosion problems to cover the lifetime problem of corroded pressure vessels.

Under this theoretical framework, we will use valid test data and data processing techniques to verify the existing corrosion models and select a more appropriate one. In addition, we employ mathematical techniques to establish time-varying failure criteria. Our goal is to obtain a new

Preprints (www.preprints.org) | NOT PEER-REVIEWED | Posted: 7 October 2023 doi:10.20944/preprints202310.0407.v1

analytical method and use it to predict the lifetime of pressured elastic spherical shells with mechanically-assisted corrosion much better. This new method will likely meet the higher demand for security assessments or regular inspections in new applications.

In the next Section 2 of the paper, we introduce the problem formulation. Section 3 is devoted to solving this formulation to obtain a new analytical method. Section 4 will address case studies of particular interest to showcase the solution's predictive capabilities. The last section summarizes and discusses our findings.

2. Problem formulation

2.1. Characterization of shell state

We know that the boundary state can theoretically characterize the state of the shell $S(t)$ (including stress and geometry) and can be described by the state of the mass point on the inner surface, $B_i(t)$. Therefore, we can choose any point M on the inner boundary of the shell as the research object as shown in Figure 1. The purpose is to obtain the spatial position (h, r_c) of this point and the associated stress stress $\sigma(t)$ in time, and then to obtain $h^*, t^*$of the shell which is in a critical state of failure.

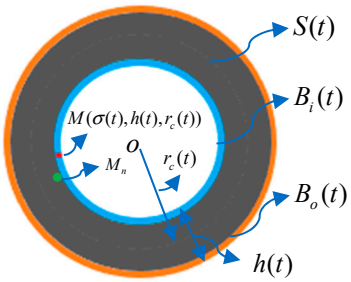

Figure 1. Characterization for shell S, boundary B and a trajectory of a point M lying at the boundary.

As the corrosion progresses, the boundary points (such as M) may dissolve in the next moment, and the new interior points (such as M_n) will become new boundary points.

2.1.1. For solving h and r_c {Solution of the problem for stresses}

Following the predecessors' practice, this paper starts fundamentally from the accurate solution for the stress balance equation, well known as Lamé's formulas:

$$\sigma_\theta(r_i) = \frac{r_i^3}{r_o^3 - r_i^3}\left(1 + \frac{r_o^3}{2r_i{}^3}\right)P_i - \frac{r_o^3}{r_o^3 - r_i^3}\left(1 + \frac{r_i^3}{2r_i{}^3}\right)P_o, \quad (1a)$$

$$\sigma_\theta(r_o) = \frac{r_i^3}{r_o^3 - r_i^3}\left(1 + \frac{r_o^3}{2r_o{}^3}\right)P_i - \frac{r_o^3}{r_o^3 - r_i^3}\left(1 + \frac{r_i^3}{2r_o{}^3}\right)P_o. \quad (1b)$$

Firstly, in order to help decoupling differential equations later, we introduce a new intermediate variable, x: x=h/r_c. Then, using x to rewrite Lamé's equation [37] and also conduct Taylor expansion considering x is typically less than unity, we obtain:

$$\sigma_\theta(r_i) = \left[\left(\frac{1}{2x} - \frac{x^2}{48} - \frac{1}{4} + \frac{3x}{8}\right)P_i - \left(\frac{1}{2x} + \frac{x^2}{16} + \frac{3}{4} + \frac{3x}{8}\right)P_o\right]w(x), \quad (2a)$$

and

$$\sigma_\theta(r_o) = \left[\left(\frac{1}{2x} - \frac{x^2}{16} - \frac{3}{4} + \frac{3x}{8}\right)P_i - \left(\frac{1}{2x} + \frac{x^2}{48} + \frac{1}{4} + \frac{3x}{8}\right)P_o\right]w(x). \quad (2b)$$

Here, $w(x) = 1/\left(1+\frac{x^2}{12}\right)$.

Equation (2) can be easily rewritten as:

Preprints (www.preprints.org) | NOT PEER-REVIEWED | Posted: 7 October 2023 doi:10.20944/preprints202310.0407.v1

$$\sigma_\theta(r_i) = f(x)(p_i - p_o) - \frac{p_i+3p_o}{4}, \text{ (3a)}$$

and

$$\sigma_\theta(r_o) = f(x)(p_i - p_o) - \frac{3p_i+p_o}{4}. \text{ (3b)}$$

Physically, this represents the coefficient of the time-variant thickness-to-radius ratio that describes the effect of corrosion on the effective stress of the shell under internal and external pressures.

According to existing kinetic corrosion equations [37,39], the relationship between v_i, v_o, $\sigma(r_j)$, and t is given by Equation (4).

$$v_j = \frac{dr_j}{dt} = [a_j + m_j\sigma(r_j)]e^{-bt}. \text{ (4)}$$

Considering $h(t)=r_o(t) - r_i(t)$ and $r_c(t)=[r_o(t)+r_i(t)]/2$, and substituting Equations (4) into Equation (3), gives,

$$\frac{dh}{dt} = \left\{(-a_o - a_i) + (-m_o - m_i)[f(x)\Delta p - \frac{p_i-p_o}{2}]\right\}e^{-bt}, \text{ (5a)}$$

and

$$\frac{dr_c}{dt} = \left\{\frac{(-a_o+a_i)}{2} + \frac{(-m_o+m_i)}{2}[f(x)\Delta p - (p_i + p_o)]\right\}e^{-bt}. \text{ (5b)}$$

By dividing Equation (5a) by Equation (5b) and considering the time-variant relationship between the geometric parameters r_c, h, and x, we obtain the phase trajectory of the system for the first time:

$$\frac{2(\frac{h}{x}-r_{c0})+(h_0-h)}{2(\frac{h}{x}-r_{c0})-(h-h_0)} = -\frac{a_i+m_i\left[f(x)\Delta p-\frac{p_i+3p_o}{4}\right]}{a_o+m_o\left[f(x)\Delta p-\frac{3p_i+p_o}{4}\right]}.. \text{ (6)}$$

Note, the phase trajectory expressed an important relationship between two dependent variables, h and r_c, which is founded on the new intermediate variable x ($x=h/r_c$) *distinctively* introduced in this paper.

In this study, the *t-h* relationship is re-obtained based on a combination of Equations (3a) and (6). Whether numerical or analytical solutions can be obtained simultaneously depends on the assumptions made.

Previous studies have always assumed that $r_c=r_{c0}$ [32,33] (that is, r_c is no longer a time-varying physical quantity) to achieve decoupling of r_c from time t simply, and accordingly, r_c is decoupled of from h and σ simultaneously. However, in this paper, we would like to remain in the time-varying field to solve this moving boundary problem in a much more general way, aiming to obtain its analytical solution. Considering that x is small (always less than 1.0), we can ignore the higher-power terms x and ax^2, and then establish a new expression of phase trajectory (Equation (6)) smoothly,

$$x = \frac{-e}{b+c/r_{co}+d/h}. \text{ (7)}$$

Employing Equation (7), we can solve Equation (5a) and Equation (5b) to obtain the expressions for h and r_c.

2.1.2. For solving σ(t)

We would follow the basic formulation of Lamé as

$$\sigma_\theta(r_i) = \frac{r_i^3}{r_o^3-r_i^3}\left(1+\frac{r_o^3}{2r_i{}^3}\right)P_i - \frac{r_o^3}{r_o^3-r_i^3}\left(1+\frac{r_i^3}{2r_i{}^3}\right)P_{,o} \text{ (8a)}$$

$$\sigma_\theta(r_o) = \frac{r_i^3}{r_o^3-r_i^3}\left(1+\frac{r_o^3}{2r_o{}^3}\right)P_i - \frac{r_o^3}{r_o^3-r_i^3}\left(1+\frac{r_i^3}{2r_o{}^3}\right)P_o. \text{ (8b)}$$

and could get the differential naturally [33], which is widely regarded as the most accurate solution and often used as the reference method,

Preprints (www.preprints.org) | NOT PEER-REVIEWED | Posted: 7 October 2023 doi:10.20944/preprints202310.0407.v1

$$\frac{d\sigma}{dt}=\left\{\frac{2}{\Delta pr_c}(\sigma+\delta)^2(\tilde{a}+m\sigma)+\frac{\sigma+\delta}{2r_c}(\bar{\tilde{a}}+\bar{\tilde{m}}\sigma)\right\}e^{-bt}. \quad (9)$$

We rewrite Equation (9),

$$\frac{d\sigma}{dt}=(\Delta_1+\Delta_2+\Delta_3)e^{-bt},$$

where:

$$\Delta_1=\frac{2}{\Delta pr_c}(\sigma+\delta)^2(\tilde{a}+m\sigma),$$

$$\Delta_2=\frac{\bar{\tilde{m}}m}{\Delta pr_c{}^2}(\sigma+\delta)^2,$$

$$\Delta_3=\frac{\sigma+\delta}{2r_c}(\bar{\tilde{a}}+\bar{\tilde{m}}\sigma)-\frac{\bar{\tilde{m}}m}{\Delta pr_c{}^2}(\sigma+\delta)^2,$$

here, $\tilde{a}=a_i+a_o-m_o\Delta P/2, m=m_i+m_o$, $\bar{\tilde{a}}=a_i-a_o+m_o\Delta P/2$, $\bar{\tilde{m}}=m_i-m_o$, $\delta=(p_i+3p_o)/4$, and $\Delta p=p_i-p_o$.

For solving σ, an assumption Δ_2,Δ_3=0 has already been employed in the method of [33].

In this paper, we would like to retain one more and put forward a new assumption,

$$\Delta_3=0. \quad (10)$$

From a formula truncation view, this assumption abandons fewer items, therefore, in theory must be more accurate. Thus, we confidently hold on that it will help acquire a more accurate solution than before, promising an analytical one if fortunate.

Then we get a new differential form as,

$$\frac{d\sigma}{dt}=(\Delta_1+\Delta_2)e^{-bt}. \quad (11)$$

Also, based on Equation (11), $\sigma(r_i)$ can be solved.

For the sake of brevity, we will present our results for h, r_c and $\sigma(r_i)$ straightforward below.

3. A new analytical method

3.1. Promotion of the boundary stress σ

This paper obtains the analytical expressions for the stress $\sigma(t)$ and the spatial position (h, r_c) of point M (see Figure 1). Its stress expression is:

b=0

$$t=\frac{\Delta pr_c}{2(\tilde{a}-m\delta_\sigma)}\left[\frac{m}{\tilde{a}-m\delta_\sigma}ln\frac{(\tilde{a}+m\sigma)}{(\tilde{a}+m\sigma_0)}\frac{(\sigma_0+\delta_\sigma)}{(\sigma+\delta_\sigma)}+\frac{\sigma-\sigma_0}{(\sigma+\delta_\sigma)(\sigma_0+\delta_\delta)}\right], \quad (12a)$$

$b\neq0$

$$t=1-\frac{1}{b}ln\left\{\frac{\Delta pr_c}{2(\tilde{a}-m\delta_\sigma)}\left[\frac{m}{\tilde{a}-m\delta_\sigma}ln\frac{(\tilde{a}+m\sigma)}{(\tilde{a}+m\sigma_0)}\frac{(\sigma_0+\delta_\sigma)}{(\sigma+\delta_\sigma)}+\frac{\sigma-\sigma_0}{(\sigma+\delta_\sigma)(\sigma_0+\delta_\delta)}\right]\right\}, \quad (12b)$$

here,$\tilde{a}=a_i+a_o-m_o\Delta p/2+(m_i-m_o)(m_i+m_o)/2/r_c$.

Note that Equation (12) are practically identical to those in [33] where in Equation (14), only parameter $\tilde{a}$ is different ($\tilde{a}=a_i+a_o-m_R\Delta p/2$).

3.2 Improvement of the vessel thickness h

At the same time, the analytical formula for the thickness h at point M is also obtained as follows:

b=0

$$t=\frac{(h_0-h)}{A}+\frac{B}{A^2}ln\frac{Ah+B}{Ah_0+B}, \quad (13a)$$

$b\neq0$

$$t=-\frac{1}{b}ln\left\{1-b[\frac{(h_0-h)}{A}+\frac{B}{A^2}ln\frac{Ah+B}{Ah_0+B}]\right\}, \quad (13b)$$

Preprints (www.preprints.org) | NOT PEER-REVIEWED | Posted: 7 October 2023 doi:10.20944/preprints202310.0407.v1

where, $A = -a_o - a_i + m_o\frac{3p_i+p_o}{4} + m_i\frac{p_i+3p_o}{4} + \frac{1}{2}(p_i - p_o)(m_o + m_i)\frac{b_1+c/r_{c0}}{e}$, $B = -\frac{1}{2}(p_i - p_o)(-m_o - m_i)\frac{d}{e}$.

Here, $a = -2\left(a_i - a_o - m_i\frac{p_i+3p_o}{4} + m_o\frac{3p_i+p_o}{4}\right)$, $b_1 = 4(p_i m_o + p_o m_i - a_i - a_o)$, $c = 2h_0\left(a_i - a_o - m_i\frac{p_i+3p_o}{4} + m_o\frac{3p_i+p_o}{4}\right) + 4r_{co}\left(a_i + a_o - m_i\frac{p_i+3p_o}{4} - m_o\frac{3p_i+p_o}{4}\right) d = \left[h_0(p_i - p_o)(m_i - m_o) + 2r_{c_o}(p_i - p_o)(m_i + m_o)\right]$, and $e = -2(p_i - p_o)(m_i + m_o)$.

We would also notice that Equation (13) are identical in form to those in [33] where in Equation (12) and (13), only parameters, A and B, are different,

$$A = -a_o - a_i + m_o\frac{3p_i+p_o}{4} + m_i\frac{p_i+3p_o}{4}, B = \frac{r_{c0}}{2}(p_i - p_o)(-m_o - m_i).$$

3.3. Presentation of the vessel mid-surface radius r_c in time

Finally, we obtain the analytical formula of the mid-plane radius r_c in time at the point M for the first time as follows:

b=0

$$t = -\frac{(r_{c_0} - r_c)}{A} + \frac{B}{A^2} ln\frac{Ar_c + B}{Ar_{c_0} + B}, \quad (14a)$$

b≠0

$$t = -\frac{1}{b} ln\left(1 + b\left(\frac{(r_{c_0} - r_c)}{A} + \frac{B}{A^2} ln\frac{Ar_c + B}{Ar_{c_0} + B}\right)\right), \quad (14b)$$

where: $A = (-a_o + a_i - m_o\frac{3p_i+p_o}{4} - m_i\frac{p_i+3p_o}{4})/2 + \frac{1}{4}(p_i - p_o)(m_o - m_i)\frac{b_1+c/r_{c0}}{e}$, and $B = \frac{1}{4}(p_i - p_o)(m_o - m_i)\frac{d}{e}$.

Equation (14) shows a non-monotonic relationship between the function r_c and time t. In other words, r_c is a nonlinear time variable. It is easy to foresee that this solution will theoretically maintain accuracy over the long-term domain. Conversely, if r_c is simply assumed to be a non-time variable, r_{c0}, as in [33], it will not.

3.4 Additional interesting finding

Additionally, there is an interesting finding that our analytical solutions for h (see Equation (13) and r_c (se Equation (14) are quite similar in form but two term signs (positive or negative) and coefficient expressions (A and B) are different.

4. Case studies

In this Section, the ability to calculate stress, σ, and tracking the spatial position (h, r_c) at the point M in a particular case, and also in general cases are verified one by one.

The method [39] is chosen as reference method for the reason mentioned in Section 2.2.2. The corresponding predicting errors by our method are delivered together with ones from existing methods [27,33].

These error formulations are defined here in advance. e_i^j represents the error for i quantity by the method j compared with reference value. Here, i could be σ, h, r_c, h^*, t^*, while j will take the values W, P or G. W represents results by this method; R represents reference value by [38]; P represents results by [33]; G represents results by [27]). $d_i^{(\mathrm{W,P})}$ represents the difference between h value predicted by method W and that by method P.

For example:

$$e_h^W = \frac{h^{(W)} - h^{(R)}}{h^{(R)}}, \quad d_h^{(\mathrm{W,P})} = \frac{h^{(P)} - h^{(W)}}{h^{(P)}}.$$

Preprints (www.preprints.org) | NOT PEER-REVIEWED | Posted: 7 October 2023 doi:10.20944/preprints202310.0407.v1

4.1. Tracking vessel σ and (h, r_c) in special case

A thin-shell vessel model with an identical internal and external corrosion intensity, no corrosion inhibition and with smaller internal or external pressures, such as wearable device components [9,10], is chosen as a special case, as employed in [33] (see Case 1). Case 1: $[p_c]$, $[l_c]$, $[t_c]$ below mean an international measure system unit for pressure, lenth, and time, which expression is also adopted by other literatures [26]. And here $|\Delta p|$, p_i, p, p_o, $p, |\sigma^*|, r_{i0}$, r_{o0}, λ, a_o, a_i, m_o, m_i, b can refer to the notation list in this paper.

$|\Delta p| = 3[p_c]$, p_i=15$[p_c]$, p_o=12$[p_c]$, $p = \min\{p_i, p_o\}$, $|\sigma^*| = 300[p_c]$,$r_{i0} = 78[l_c]$, $r_{o0} = 82[l_c]$, λ =0.05, $a_o = a_i = 0.1[l_c/t_c]$, $m_o = m_i = 0.0005[l_c/t_c p_c]$, b=0.

The results by the proposed method are shown in the figures below.

As can be seen from Figure 2, the σ errors predicted by methods W and P are very close. The former has only a slight advantage over the latter. This law also holds true when predicting thickness, and the error of method G is the largest, as shown in Figure 3.

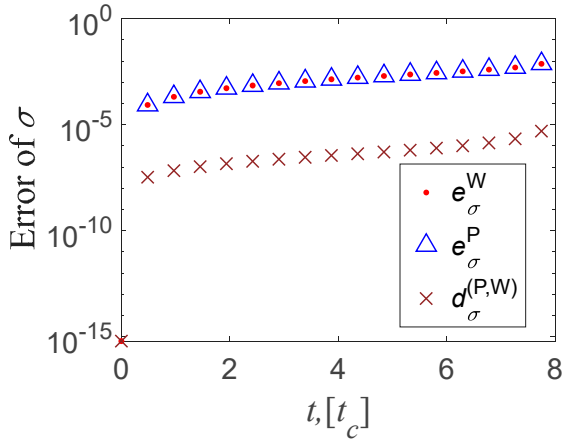

Figure 2. Stress error (difference) between methods e_σ^W,e_σ^P and $d_\sigma^{(P,W)}$.

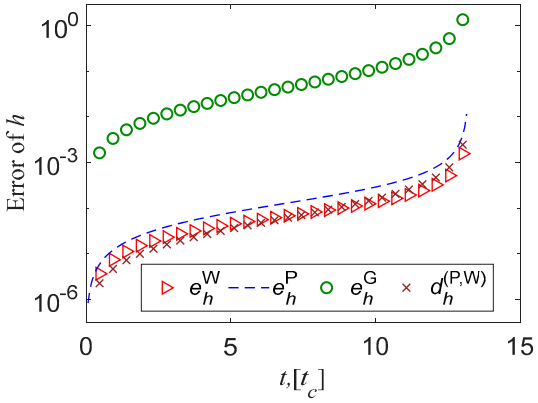

Figure 3. Thickness error (difference) between methods e_h^W,e_h^P,e_h^G and $d_h^{(P,W)}$.

As can be seen from Figure 4, for the value of the predicted mid-surface radius, in this time domain, the orders of magnitude of the prediction error by the three methods are all very small. Among them in this method is consistent with the reference solution best, and its accuracy is the highest.

Preprints (www.preprints.org) | NOT PEER-REVIEWED | Posted: 7 October 2023 doi:10.20944/preprints202310.0407.v1

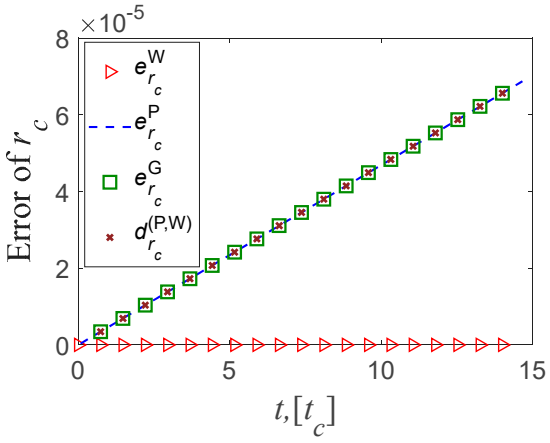

Figure 4. Mid-surface radius error (difference) between methods $e_{r_c}^{W}$,$e_{r_c}^{P}$,$e_{r_c}^{G}$and $d_{r_c}^{(P,W)}$

In general, the errors of σ and (h, r_c) predicted by this method and the existing two methods are all very small. Among them, the error of this method is the smallest, though its superiority is weak.

4.2. Tracking the h at point M under the general case

Unlike Case 1, in engineering applications such as chemical building components [6], marine platform components [7], etc., the more common physics phenomenon is that the internal and external corrosion intensity is rarely equal, the corrosion inhibition is functioning, and vessel itself is being not very thin. In order to research a more general model, we propose a new case with a different internal and external corrosion strengths, non-zero corrosion inhibition, and thicker geometric dimensions, see Case 2. Its results are shown in Figure 5.

Note that, the solution expression and its calculating for thickness and radius resemble, only results for the former are delivered here for simplicity.

Case 2:

Here $|\Delta p|$, p_i, p_o, p, $|\sigma^*|$,r_{i0}, r_{o0}, λ, a_o, a_i, m_o, m_i, b and v *can refer to the notitation list in this paper.*

$p_o = 210[p_c]$, $p_i = 10[p_c]$, $\lambda = 0.3$, $h_0 = 10[l_c]$, $a_o = 0.001[l_c/t_c\ ]$, $a_i = 0.004[l_c/t_c\ ]$, $m_o = 0.004\left[\frac{l_c}{t_c p_c}\right]$, $m_i = 0.0016\ [l_c/t_c p_c]$,b=0.001, $E = 206000[p_c]$, $v = 0.3$.

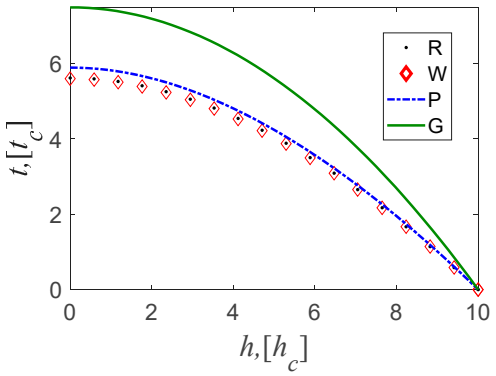

Figure 5. h-t curves traced by R, W, P, and G method.

As shown in Figure 5, the *t-h* curve predicted by our method almost coincides with the reference curve. Its accuracy is the highest, followed by [33], and the [27] method is the lowest.

Preprints (www.preprints.org) | NOT PEER-REVIEWED | Posted: 7 October 2023 doi:10.20944/preprints202310.0407.v1

4.3. Tracking vessel boundary Bi and shape S under the general case

For other common engineering applications, such as oil (gas) pipelines [5] or high temperature furnace devices [4], we seek to understand the difference of the vessel's boundary position and shape predicted by the proposed method and other methods. With the intention of well describing this situation, we set another general example, see Case 3. Whereas, unlike Case 2, its internal corrosion intensity is higher than the external one. Corresponding results are exhibited in Figures 6 and 7.

Case 3:

Here p_o, p_i, λ,h_0, a_o, a_i, m_o, m_i, b, E and v can *refer to the notitation list in this paper.*

$p_o = 15[p_c]$, $p_i = 180[p_c]$, $\lambda = 0.25$, $h_0 = 10[l_c]$, $a_o = 0.001[l_c/t_c\ ]$, $a_i = 0.02[l_c/t_c\ ]$, $m_o = 0.0004\left[\frac{l_c}{t_c p_c}\right]$, $m_i = 0.008\ [l_c/t_c p_c]$,$b$=0.01,$E = 206000[p_c]$, $v = 0.3$.

From Figure 6 we note that the accuracy of tracking thickness by this method is highest. Consequently, we can quickly obtain the thickness predicted by each method at any time t_k ($0<t_k<t^*$); in the same way we could also obtain r_c. Then we can qualitatively draw the position of boundary B and the shape of shell S at time t_k as shown in Figure 7.

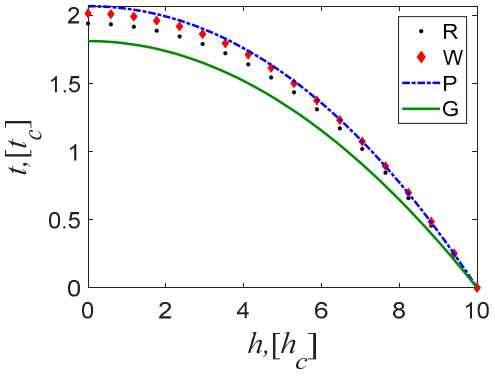

Figure 6. *h*-*t* curves traced by P,W,P, and G method.

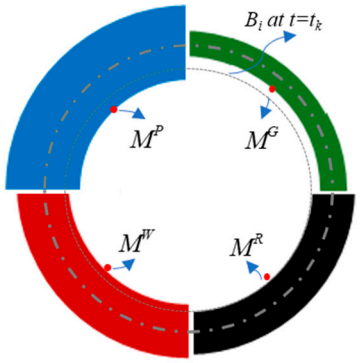

Figure 7. Qualitative geometric shape of *S*, B_i and *M*.

Note: Red represents results by this method; Black represents reference value by [35]; Blue represents results by [33]; Green represents results by [27]).

Figure 7 shows the significant differences among the three methods in tracking M positions (h, r_c). M^G is tracked by [27] method. However, at t_k it is not a real boundary point, but an interior one. M^P and M^W is tracked by method in [33] and this method respectively. However, the two positions have already dissolved and disappeared at t_k. Nevertheless, the M^W by this method is the closest to the reference value.

Preprints (www.preprints.org) | NOT PEER-REVIEWED | Posted: 7 October 2023 doi:10.20944/preprints202310.0407.v1

4.4. Predicting the shell critical state (t^*, h^*)

In some engineering applications, for example, aerial vehicles [2], or liquid hydrogen transportation pipelines [3], vessel pressure load is often relatively large, perhaps with a high corrosion inhibition, unlike case 2 and 3. It is particularly important and necessary for practitioners or operators to accurately forecast the service life of vessels in such a working condition. With this in mind, we introduce a further example as case 4. The related results are demonstrated in Figure 8 and Table 1.

Case 4

Here p_o, p_i, λ, h_0, a_o, a_i, m_o, m_i, b, E and v can refer to the notitation list in this paper.

$p_o = 15[p_c]$, $p_i = 950[p_c]$, $\lambda = 0.3$, $h_0 = 10[l_c]$, $a_o = 0.004[l_c/t_c\ ]$, $a_i = 0.001[l_c/t_c\ ]$, $m_o = 0.0016\left[\frac{l_c}{t_c p_c}\right]$, $m_i = 0.0004\ [l_c/t_c p_c]$, $b = 0.455, E = 206000[p_c]$, $v = 0.3$.

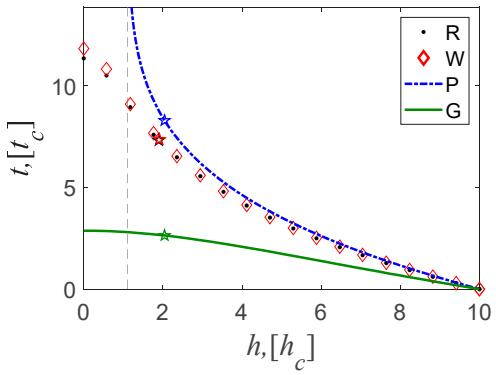

Figure 8. *h-t* curves and their *t**, *h** traced by R,W,P,and G method.

Figure 8 shows the four *h-t* curves predicted by different methods. The curve of this method is almost consistent with the reference method, indicating that this method has the highest accuracy, and the higher one results from the [33] method. The lowest level of agreement is seen from the [27] method.

Let us note that in the curve of [33], *t* tends to positive infinity when *h* approaches 1.14 [*l*c]. This phenomenon shows that the shell will never completely dissolve (it has a remaining thickness of at least 1.14 [*l*c] no matter how much time has passed), assuming the shell has not failed before then. This suggestion is somewhat inconsistent with physical phenomena.

Table 1 shows that the error of t^* by [33] reaches 13%, which exceeds the general engineering accuracy (5%). Therefore, the lifetime it predicts is difficult to guarantee reliability. In contrast, the error of this method is less than 1%, which is lower than the general engineering accuracy, and its predicted lifetime is much more reliable and thus more useful. The error of h^* follows similarly.

Table 1. t^* error (difference) between methods $e^j_{t^*}$,$e^j_{h^*}$,$d^{(P,W)}_{t^*}$and $d^{(P,W)}_{h^*}$ (%) (*j*=W,P,G).

e_i^j or $d_i^{(P,W)}$	$e_{t^*}^W$	$e_{t^*}^P$	$e_{t^*}^G$	$d_{t^*}^{(P,W)}$
Value	0.6	13.3	70.0	12.7
e_i^j or $d_i^{(P,W)}$	$e_{h^*}^W$	$e_{h^*}^P$	$e_{h^*}^G$	$d_{h^*}^{(P,W)}$
Value	0.8	7.6	7.6	6.8

5. Conclusions

Having described the existing research methods relating to corrosion problems in pressured vessels and discussed their evolution, advantages, and disadvantages, we justified that there is a strong need for uniform corrosion analysis methods for both current and new applications. Existing methods struggle to meet this need. Accordingly, this paper proposes an improved approach with a view to addressing current needs. This novel approach was successfully implemented. The

Preprints (www.preprints.org) | NOT PEER-REVIEWED | Posted: 7 October 2023 doi:10.20944/preprints202310.0407.v1

contribution of this new method is mainly reflected in: popularizing existing methods for engineering applications, research technology for physical science, nonlinear differential equation solving methods and techniques for mathematics, etc.

5.1. Contributions to engineering applications:

The proposed method generalizes a popular method [33] in engineering applications, the promotion and improvement are as follows:

(a) Our method achieves a global, simultaneous tracking of shell shape (thickness and midplane radius) and stress. Therefore, we generalize those existing methods, which usually solve only for thickness, or only for stress.
(b) Moreover, relative to the existing methods, their respective analytical solutions are all: easy to program, not more time-consuming, operator-friendly, and more accurate. It is more widely applicable, functioning in settings with large-scale time domains and general working conditions.
(c) This general case refers to: more general corrosion conditions (internal and external corrosion rates in any ratio), pressure conditions (internal and external pressure in any ratio) or geometry (thin shell, medium-thick shell, or thick shell).
(d) Most importantly, we can obtain higher accuracy of lifetime t^* and critical thickness h^*. Note that the lifetime accuracy of the other method (P) is lower (or slightly lower) than this method in special and ordinary cases. In one of the cases, it even made a prediction that did not match the physical phenomenon (no matter how long it took, the shell could not be completely corroded). That is, in the long-term domain, its prediction of lifespan is distorted.

5.2. Contributions to research techniques in physical sciences

Taking the moving boundary problem (shell boundary/stress tracking and life prediction) as an example, this paper explores a physical science research technique that is promising to be universal. That is, how to improve the solution itself by physically improving the parameters of the solution (method) and successfully without complicating the form of the solution and the implementation of the application.

5.3. Contributions to methods and techniques for solving systems of nonlinear differential equations in mathematics

Nonlinearity is everywhere [40] (on all time and spatial scales). Many phenomena of this nonlinear excitation naturally include the failure of general corrosion of pressure vessels [41]. The problem is to solve its first-order nonlinear differential equation system (one independent variable, time; two dependent variables, r_i and r_o; and two intermediate variables, σ_i and σ_o).

Analytical solutions for such a system of equations are generally not available in mathematics [42]. In general, one can only obtain its numerical solution (by simple iteration method, Newton iteration method, Newton-Raphson method, spline function, Hermite interpolation, Lagrange interpolation, etc.), or do some qualitative analysis of it (e.g., its stability study or equilibrium point analysis) [42]. If one wants to obtain its analytical solution, one must achieve the separation of dependent and independent variables within the system of equations (or equation decoupling).

To circumvent this difficulty, the P (or G) method simply separated the independent variable (t) and the dependent variable (r_c) by assuming $r_c = r_{c0}$, thus reducing the system of equations to just one equation. An analytic solution for h could then be readily found.

Our approach is different. We first analyze the phase trajectory of the two dependent variables of this equation and obtain their explicit relationship. Then, we introduce reasonable assumptions, (e.g., ignore higher-order terms of small terms) to simplify the relationship between the two dependent variables. This simplification in turn reduces the original system of equations to one equation, which allows us to obtain its analytical solution elegantly.

Preprints (www.preprints.org) | NOT PEER-REVIEWED | Posted: 7 October 2023 doi:10.20944/preprints202310.0407.v1

During solving, this paper also proposes another mathematical technique, which is to properly introduce the intermediate variable x (x= h /r_c). This distinctive introduction plays a key role in the successful separation of the original two intermediate variables (σ_i and σ_o).

From the above, it is readily seen that by successfully solving the extremely difficult nonlinear differential equation system, we have contributed a general mathematical method (analyzing the equivalence line and obtaining the nonlinear relationship of the dependent variable) and a mathematical technique (introducing an appropriate intermediate variable, x). The successful use of both in this paper demonstrates their utility in the study of non-linear problems.

5.4. The proposed method needs further discussion

As is the case with any new method, the proposed one needs further study, in particular if one wishes to extend it for different geometries (ellipsoidal spherical shell, cylindrical shell, etc.) or introduce further features such as temperature. The authors would suggest that one employ numerical solutions, analytical solutions, and qualitative analysis (studies of stability and equilibrium) for such a study.

Funding: (1) This work was supported by the National Natural Science Foundation of China [Grant number, 52068003]. (2) The sponsorship guaranteed with basic research funds provided by Politecnico di Torino, Italy, for its financial aid in this work is also acknowledged. (3) Opinions, findings, and conclusions expressed in this paper are those of the authors and not necessarily those of the sponsors.

Acknowledgments: The author (C. H. Liu) is thankful to Department of Mathematics for hospitality during her stay at Aberystwyth University. The authors (C. H. Liu & G. Lacidogna) thank Dr A. Vellender, Dr D. Peck and Prof. G. Mishuris for fruitful discussions. The author (C. H. Liu) also thanks Dr. H.Y. Cheng in Department of Engineering Science and Mechanics of the Pennsylvania State University, Prof. I. Burgess and Dr. S. Huang in Department of Civil and Structural Engineering of the University of Sheffield, Prof S. Shi in Department of Mathematics of Hefei University of Technology for working and discussing in its earlier stage.

Notation List

A	thermal expansion coefficient of the material
a_i	corrosion constant for internal corrosion
a_o	corrosion constant for external corrosion
b	corrosion inhibition effect
dr	radius of two concentric spheres
D_θ	the angle between the plane and the positive z-axis
d_φ	angle between the x-axis counterclockwise and the plane
$f(x)$	coefficient of the time-variant thickness-to-radius ratio
h, $h(t)$	thickness
h^*	corresponding thickness of the shell under the critical failure state
h_a	given minimal allowable thickness
m_i	corrosion constant
m_o	corrosion constant
p_i	inner pressure
p_o	outer pressure
$\triangle p$	p_i - p_o
r, $r(t)$	distance between a point in the shell material and the origin of the coordinate system
r_o	distance between the internal surface in the shell material and the origin of the coordinate system
r_c,$r_c(t)$, (r_i, $r_i(t)$, r_o, $r_o(t)$	middle (inner, outer) surface radius of the shell
t	time
t^*	time required for a corroded pressure shell to fail for the first time due to buckling or yielding
t_d	time for the shell to completely dissolve
v_i (v_o)	inner (outer) mechano-chemical corrosion rate
x	thickness to mid-surface radius ratio,$x = h/r_c$, or $2(r_o - r_i)/(r_o + r_i)$ for spherical shell

σ	stress under longitudinal or transverse forces, cylindrical shells, spherical shells, or other shells
$\sigma(r_j)$	principal stress; $j = i, o$
$\sigma(r_j)_{\max}$	maximum principal stress
$\sigma_e(r)$	effective stress/ the equivalent stress
$\sigma_r(r)$	radial stress
$\sigma_\theta(r)$	hoop stress maximum hoop or simply hoop
$\sigma_\varphi(r)$	meridian stress
e_h^M $(e_{r_c}^M, e_{t^*}^M, e_{h^*}^M)$	*error of* h (r_c, t^*, h^*) predicted by method M in comparison with reference method R
$d_h^{(\mathrm{P,W})}(d_{r_c}^{(\mathrm{P,W})}, d_{t^*}^{(\mathrm{P,W})}, d_{h^*}^{(\mathrm{P,W})})$	difference between h (r_c, t^*, h^*) value predicted by method P and that by method W
$S(t)$	shell S state
$B_i(t)$ $(B_o(t))$	inner (outer) boundary of shell one line

References

1. Allen H. Corrosion Problems with Pressure Vessels. Anti-Corrosion Methods Mater.1958,5(12):390-397.
2. Czaban M. Aircraft Corrosion Review of Corrosion Processes and its Effects in Selected Cases. Fatigue Aircr Struct. 2018,10:5-20.
3. Brian P.; Somerday CSM. Effects of Hydrogen Gas on Steel Vessels and Piplelines. Brian P. Somerday and Chris San Marchi Sandia National Laboratories: Livermore, USA, 2006: pp.1-34.
4. Faes W; Lecompte S; Ahmed ZY. Corrosion and Corrosion Prevention in Heat Exchangers. Corros Rev. 2019, 37(2): 131-155.
5. Askari M; Aliofkhazraei M; Afroukhteh S. A Comprehensive Review on Internal Corrosion and Cracking of Oil and Gas Pipelines. J Nat Gas Sci Eng. 2019, 71:1-25.
6. Hashim NZN; Kassim K. The Effect of Temperature on Mild Steel Corrosion in 1 M HCL by Schiff Bases. Malaysian J Anal Sci. 2014,18(1): 28-36.
7. Liu JG; Li Z, Li Y; Hou BR. Corrosion Process of D32 Steel Used for Offshore Oil Platform in Splash zone. Anti-Corrosion Methods Mater. 2016, 63(1): 56-64.
8. MacLeod ID. Corrosion and Conservation Management of the Submarine HMAS AE2 (1915) in the Sea of Marmara, Turkey. Heritage. 2019, 2(1): 868-883.
9. Yang X; Cheng H. Recent Developments of Flexible and Stretchable Electrochemical Biosensors. Micromachines. 2020,11(243): 1-34.
10. Zhou H, Qin W, Yu Q, Yu X, Cheng H, Wu H. Circumferential Buckling and Postbuckling Analysis of Thin Films Integrated on a Soft Cylindrical Substrate with Surface Relief Structures. Extrem Mech Lett. 2020, 35: 2352-4316.
11. Yang HQ; Zhang Q; Tu SS; Wang Y; Li YM; Huang Y. A Study on Time-Variant Corrosion Model for Immersed Steel Plate Elements Considering the Effect of Mechanical Stress. Ocean Eng. 2016, 125: 134-146.
12. De Meo D; Oterkus E. Finite Element Implementation of a Peridynamic Pitting Corrosion Damage Model. Ocean Eng. 2017,135:76-83.
13. Cui C; Ma R. Martínez-Pañeda E. A Phase Field Formulation for Dissolution-Driven Stress Corrosion Cracking. J Mech Phys Solids. 2021,147:104254-104275.
14. Kristensen PK; Niordson CF. Martínez-Pañeda E. An Assessment of Phase Field Fracture: Crack Initiation and Growth. Philos Trans R Soc A Math Phys Eng Sci. 2021, 379: 2203-2245.
15. Kristensen PK; Niordson CF. Martínez-Pañeda E. Applications of Phase Field Fracture in Modelling Hydrogen Assisted Failures. Theor Appl Fract Mech. 2020, 110: 1-13.
16. Jivkov AP. Deformation-Promoted Nucleation of Corrosion Cracks: State, Problems and Perspectives. 2003, 44(0):1-17.
17. Gutman EM; Zainullin RS; Zaripov RA. Kinetics of Mechanicochemical Failure and the Life of Constructional Elements in Tension in Elastoplastic Deformations. Sov Mater Sci. 1984, 20(2): 101-103.
18. G.V. Akimov. Fundamentals of the Corrosion Theory and Metal Protection, Metallurgizdat: Moscow, Russia,1964; pp. 24–56.
19. Dolinskii, V. M. Calculations on Loaded Tubes Exposed to Corrosion. Chem Pet Eng.1967,3(2): 96–97.
20. E.M. Gutman; R. S. Zainullin; R. A. Zaripov. The Life of High-pressure Vessels under Conditions of Mechanicochemical Corrosion, in: Corrosion and Protection in the Petroleum and Gas Industry. Vsesoyuz. Nauch. -Isled. Inst. Org.: Promysh, Russia,1977; pp. 3-5.
21. E.M. Gutman. The Mechanical Chemistry of Metals and Protection from Corrosion, Metallurgiya, Moscow,1981; pp. 90–120.

22. Gutman EM. Mechanochemistry of Solid Surfaces. Mechanochemistry of Solid Surfaces: World Scientific,Singapore, Singapore,1994; pp. 1–80
23. Elishakoff I; Ghyselinck G; Miglis Y. Durability of an Elastic Bar under Tension with Linear or Nonlinear Relationship between Corrosion Rate and Stress. J Appl Mech Trans ASME. 2012,79(2): 1-8.
24. Pavlov PA; Malibekov AK. Multicycle Fatigue of Carbon Steels. 1987, (8): 41-45.
25. Pronina Y; Sedova O. Analytical Solution for the Lifetime of a Spherical Shell of Arbitrary Thickness under the Pressure of Corrosive Environments: The Effect of Thermal and Elastic Stresses. J Appl Mech Trans ASME. 2021;88(6):61004-61013.
26. Pronina YG. Analytical Solution for Decelerated Mechanochemical Corrosion of Pressurized Elastic-perfectly Plastic Thick-walled Spheres. Corros Sci. 2015, 90:161-167.
27. Gutman EM; Bergman RM; Levitsky SP. Influence of Internal Uniform Corrosion on Stability Loss of a Thin-walled Spherical Shell Subjected to External Pressure. Corros Sci. 2016,111: 212-215.
28. Gutman EM. An inconsistency in Film Rupture Model of Stress Corrosion Cracking. Corros Sci. 2007,49(5): 2289-2302.
29. Gutman E; Haddad J; Bergman R. Stability of Thin-walled High-pressure Vessels Subjected to Uniform Corrosion. Thin-Walled Struct. 2000, 38(1): 43-52.
30. Gutman EM; Haddad J; Bergman R. Stability of Thin-walled High-pressure Cylindrical Pipes with Non-circular Cross-section and Variable Wall Thickness Subjected to Non-homogeneous Corrosion. Thin-Walled Struct. 2005;43(1): 23-32.
31. Bergman RM; Levitsky SP; Haddad J; Gutman EM. Stability Loss of Thin-walled Cylindrical Tubes, Subjected to Longitudinal Compressive Forces and External Corrosion. Thin-Walled Struct. 2006, 44(7):726-729.
32. Pronina Y; Sedova O; Grekov M; Sergeeva T. On Corrosion of a Thin-walled Spherical Vessel under Pressure. Int J Eng Sci. 2018,130: 115-128.
33. Alfutov, N.A. Stability of Shells. In: Stability of Elastic Structures. Foundations of Engineering Mechanics. Springer, Berlin, Germany, 2000; pp. 221–285.
34. Liu H; Yuan H; Zhang W. Time-varied Stability Loss of Uniformly Compressed Hemispherical Shells Subjected to Uniform Corrosion Based on the Southwell Procedure. In Proceedings of IASS Annual Symposia, Boston, USA,16th July 2018.
35. Liu CH; Lacidogna G. A Non-Destructive Method for Predicting Critical Load, Critical Thickness and Service Life for Corroded Spherical Shells under Uniform External Pressure Based on NDT Data. Appl Sci. 2023;13(7): 4172-4191.
36. Timoshenko, S. P.; Gere, J. M. Theory of elastic stability. Dover Publications: New York, USA, 2009.
37. Vol'mir, A. S. Stability of Deformable Systems. Fizmatlit, Moscow, Russia,1970.
38. Pronina, Y. G.; Sedova, O. S.; Kabrits, S. A. On the Applicability of Thin Spherical Shell Model for the Problems of Mechanochemical Corrosion. AIP Conf. Proc. 2015,1648:1–5.
39. Campbell, David K. Nonlinear physics: Fresh breather. Nature. 2004; 432 (7016): 455–456.
40. Jordan, D. W.; Smith, P. Nonlinear Ordinary Differential Equations. The Mathematical Gazette. 1979,63,1-66.
41. Daniel Lazard. Thirty years of Polynomial System Solving, and now? Journal of Symbolic Computation. J Symb. Comput. 2009,44(3): 222-231.